DEUTSCHES ELEKTRONEN-SYNCHROTRON DESY

Higher Order Leading Logarithms and
Evaluation in Deep Inelastic Scattering
at Very High Energies

M. Klasen
Deutsches Elektronen-Synchrotron DESY
II. Institut für Theoretische Physik, Universität Hamburg

DESY 96-177
August 1996

NOTKESTRASSE 85 - 2 HAMBURG 52

Dr. Ing. h.c. F. Porsche AG
Porscheplatz 1
70435 Stuttgart
Germany

DESY 90-096
August 1990

ISSN 0418-9833

Higher order leading logarithmic QED corrections to deep inelastic ep scattering at very high energies

J. Kripfganz, H.-J. Möhring

Sektion Physik, Karl-Marx-Universität Leipzig,

Karl-Marx-Platz 10-11, DDR-7010 Leipzig

H. Spiesberger*

II. Institut für Theoretische Physik der Universität Hamburg,

Luruper Chaussee 149, D-2000 Hamburg 50, Germany

Abstract

Higher order electromagnetic radiative corrections to neutral current deep inelastic electron proton scattering are studied in collinear approximation. Second order corrections show qualitatively new features compared to the first order ones and are non-negligible for large y and small x. We also show how kinematical cuts on the recoil quark jet, in particular the jet angle, will allow a strong reduction of the contribution from radiative events for small x and large y.

*Supported by Bundesministerium für Forschung und Technologie, 05 5HH91P (8), Bonn, FRG

1. Introduction

Deep inelastic lepton nucleon scattering provides an important tool for studying the internal structure of nucleons. The HERA machine will extend the energy range accessible for ep scattering considerably: electron and proton beams of 30 and 820 GeV, resp., will allow measurements at Q^2 values up to several $10^4\,GeV^2$ and x values down to 10^{-4} [1]. High-precision measurements of structure functions and tests of the electroweak standard model, as well as the possibility of observing new phenomena require a detailed understanding of the standard model predictions.

To first order in α, complete calculations of the electroweak corrections for the neutral current process within the standard model were performed independently by two groups [2,3]. Their results agree numerically within 0.5% for the kinematical range $0.02 \leq x, y \leq 0.98$. Recently these results have been confirmed by calculations performed in the leading logarithmic approximation [4,5] as well as with the help of a Monte Carlo event generator [6].

The $\mathcal{O}(\alpha)$ corrections for NC scattering are large for small x and large y. These large corrections originate from bremsstrahlung from the lepton line plus corresponding virtual contributions (Fig. 1, leptonic corrections). Other $\mathcal{O}(\alpha)$ contributions lead in general to much smaller effects. There are two reasons for the importance of these leptonic corrections: *i*) Their order of magnitude is determined by a large logarithm of the electron mass $\ln(Q^2/m_e^2)$, and *ii*) the emission of energy via bremsstrahlung from the electron line, particularly in direction of the electron beam, can shift the effective momentum transfer at the quark line $\hat{Q}^2 = -(p_e - p_e' - k)^2$ to values much smaller than the momentum transfer $Q^2 = -(p_e - p_e')^2$ measured from the momentum of the outgoing electron: $\hat{Q}^2 \ll Q^2$. This leads to an enhancement of the cross section for radiative events. The minimal value of $\hat{Q}^2$ that can be reached by the emission of a photon is determined by the proton mass. Therefore there is also an important part of the leptonic corrections which is not determined by a logarithm of the electron mass, but instead by a logarithm of a hadronic mass scale. This part, which is contained in the first two diagrams of Fig. 1 (describing photon exchange), can be viewed as arising from collinear photon emission from the quark line, followed by Compton scattering $e\gamma \to e\gamma$. Its contribution is significant at large y and small x because of the backward peak of the Compton cross section.

The mass singularities of the leptonic corrections can be separated into parts that may be associated to the external fermion lines. There are mass singularities pertaining to the incoming as well as to the outgoing electron line, but also to the incoming hadron line. In a parton model language these separate parts correspond to structure functions for the external fermions that describe the emission of photons, fermions,

etc. The mass singularities arising from the Feynman diagrams of Fig. 1 are visualized in Fig. 2. The first two contributions (Fig. 2a,b) produce electron mass singularities $\ln(Q^2/m_e^2)$ which have to be included explicitly. The remaining contributions would generate quark mass singularities which should however be absorbed into the hadronic structure functions.

The fact that $\mathcal{O}(\alpha)$ electromagnetic corrections are large obviously requires the investigation of higher order contributions. For such a purpose it is helpful to realize that the exact $\mathcal{O}(\alpha)$ corrections can be well reproduced for not too small Q^2 by a collinear approximation [4,5]. Therefore, a leading collinear approximation should be appropriate for a study of higher order contributions as well. It is the aim of this paper to supply the formulas that are relevant for the calculation of corrections up to order $\mathcal{O}(\alpha^2)$ and to study the effects to be expected numerically.

In the parton model, deep inelastic scattering is described by a sum over electron-quark hard scattering subprocesses

$$d\sigma(eP \to eX) = \sum_f \int dx' D_{q_f/P}(x') d\hat{\sigma}(eq_f \to eX) \qquad (1)$$

where $D_{q_f/P}(x')$ is the probability distribution of a quark with flavor f inside the proton, and $d\hat{\sigma}$ is the cross section for the corresponding electron quark scattering with rescaled center-of-mass energy. Leading logarithmic QCD corrections are taken into account by the introduction of Q^2 dependent parton distributions $D_{q_f/P}(x, Q^2)$. This Q^2 dependence, controlled by Gribov-Lipatov-Altarelli-Parisi evolution equations [7,8], is a remnant from absorbing mass singularities into the structure functions. Non-leading QCD corrections lead to modified evolution equations for the parton densities, as well as to finite higher order contributions to the parton cross sections. In particular, new subprocesses involving gluons will appear and Eq. (1) will receive a contribution which contains the gluon distribution.

The modification of the electron-proton cross section by electroweak corrections can be described with the help of a generalization of the parton model relation Eq. (1) [9][1]:

$$d\sigma(eP \to eX) = \sum_{a,b,c} \int dz_1 D_{a/e}(z_1) \int dz_2 D_{b/P}(z_2) \int dz_3 \tilde{D}_{e/c}(z_3) d\hat{\sigma}(ab \to cX). \qquad (2)$$

$D_{a/e}(x)$ is the density of a 'QED parton' a inside the incident electron ($a = e^+$, e^-, $\gamma, \cdots, u, \bar{u}, \cdots$), $D_{b/P}(x)$ is the distribution of parton b (including the photon) inside the proton, and $\tilde{D}_{e/c}(z_3)$ describes the fragmentation of the QED parton c into the observed final state electron. Singular parts of the electromagnetic corrections

[1] This formalism of describing electromagnetic corrections in terms of structure functions has already been used extensively for electron positron annihilation, see [10] and references therein.

can be collected into the (process independent) structure functions whereas finite contributions modify the parton subprocess cross sections $d\hat{\sigma}(ab \to cX)$. From the analogy to QCD corrections, two important properties of the QED corrections are then understandable: *i*) corrections describing bremsstrahlung from the quark line (which are not considered in this work) also modify the Q^2 dependence of the parton distribution functions and *ii*) the photon appears as a hadron constituent, too, with $e\gamma$ Compton scattering as the corresponding subprocess in Eq. (2).

The leading second order parton model diagrams are shown in Fig. 3. A qualitatively new effect appears in this order. Using a QCD terminology this would be described as the appearance of a 'sea' component of the electron structure function, *i.e.* a $1/x$ term. It corresponds to the production of an e^+e^- pair where the secondary electron undergoes the hard scattering (Fig. 3f). Additionally, fermion pairs may be radiated from the electron line in this order (Fig. 3e). Predominantly, these fermion pairs will be produced in forward direction and would be hard to observe. Logarithms of the fermion masses arising from these diagrams cancel partly against logarithms of the same type coming from the $\mathcal{O}(\alpha^2)$ diagram describing a vacuum polarization insertion in the one-loop vertex correction. Therefore we include these parts as a contribution to the $\mathcal{O}(\alpha^2)$ corrected inclusive eP cross section. Our numerical investigations show that the inclusion of $\mathcal{O}(\alpha^2)$ electromagnetic radiative processes still increases the corrections in the large y region considerably.

It has already been demonstrated in Ref. [11] that the high y peak could be removed completely if the corresponding photons could be tagged. It should be easily possible to separate the Compton contribution to the high y peak by experimental cuts. The events pertaining to this part have a clear experimental signature: the transverse momentum of the electron is essentially balanced by a hard photon. In contrast to this, direct measurements of the small-angle hard photons are presumably not feasible. It has, however, been pointed out in Ref. [12] that cuts in the angle of the recoil quark jet should allow to remove such hard photon events very efficiently. This will be demonstrated in detail in Chapter 3. This method will work at very small x as well, where without cuts very large electromagnetic corrections would have to be applied over the whole y range.

This paper is organized in the following way: In Section 2 we define our notations and provide the $\mathcal{O}(\alpha)$ and $\mathcal{O}(\alpha^2)$ expressions in leading logarithmic approximation. The $\mathcal{O}(\alpha^2)$ contributions include two-photon radiation, fermion pair production and the leptonic $\mathcal{O}(\alpha)$ correction to the Compton part of the $\mathcal{O}(\alpha)$ corrections. In the final Section 3 we discuss numerical results. We emphasize the possibility of removing large corrections by imposing suitable experimental cuts, in particular on the jet angle. Although we concentrate on the machine parameters of HERA, several results are also

given for the conditions of a possible future lepton-hadron collider in the LEP tunnel (50 GeV electrons on 8 TeV protons).

2. Factorization of mass singularities

Up to $\mathcal{O}(\alpha^2)$ the contributions to Eq. (2) describing electromagnetic radiative corrections originate from either electron-quark or electron-photon hard subprocesses. For the cross section differential in x and y this equation reads:

$$\frac{d^2\sigma}{dxdy} = \sum_{b=q,\bar{q},\gamma} \int_0^1 \frac{dz_1}{z_1} D_{e/e}(z_1) \int_0^1 \frac{dz_2}{z_2} D_{b/P}(z_2) \int_0^1 \frac{dz_3}{z_3^2} \bar{D}_{e/e}(z_3) \frac{y}{\hat{y}} \frac{d^2\hat{\sigma}}{d\hat{x}d\hat{y}}(eb \to eX) \quad (3)$$

In the following the 4-momenta of the incoming (outgoing) electron are denoted by p_e (p'_e), that of the nucleon by P_n. The momentum fractions z_i define the 4-momenta of the generalized partons in the corresponding hard subprocesses according to the convention

$$\hat{p}_e = z_1 p_e, \quad \hat{p}_b = z_2 P_n, \quad \hat{p}'_e = \frac{1}{z_3} p'_e. \quad (4)$$

As usual we introduce the kinematical variables

$$Q^2 = -(p_e - p'_e)^2, \quad x = \frac{Q^2}{2P_n(p_e - p'_e)}, \quad y = \frac{P_n(p_e - p'_e)}{P_n p_e} = \frac{Q^2}{xS} \quad (5)$$

with $S = (p_e + P_n)^2$. $\hat{S}, \hat{x}, \hat{y}$ and $\hat{Q}^2$ denote the corresponding variables for the hard electron-parton subprocesses.

$$\hat{S} = z_1 z_2 S, \quad \hat{x} = \frac{z_1 xy}{z_2(z_1 z_3 + y - 1)}, \quad \hat{y} = \frac{z_1 z_3 + y - 1}{z_1 z_3}, \quad \hat{Q}^2 = \frac{z_1}{z_3} Q^2. \quad (6)$$

In the following we assume $m_f^2 \ll S$, Q^2 and neglect fermion masses where possible.

In leading logarithmic approximation it is sufficient to use the hard-scattering cross section $d\hat{\sigma}(eb \to eX)$ in lowest order of α since the large logarithms are provided by the structure functions. The Born term for unpolarized electron-quark scattering is given by

$$\frac{d^2\hat{\sigma}^{(0)}}{d\hat{x}d\hat{y}}(e^-q \to e^-q) = \frac{2\pi\alpha^2}{\hat{x}^2\hat{y}^2\hat{S}} \left(A^f[1 + (1-\hat{y})^2] \pm B^f[1 - (1-\hat{y})^2] \right) \delta(1-\hat{x}) \quad (7)$$

where the plus and minus signs refer to quark and antiquark scattering, resp., and

$$\begin{aligned} A^f &= e_f^2 - 2v_e e_f v_f \chi_Z(\hat{Q}^2) + (v_e^2 + a_e^2)(v_f^2 + a_f^2) \left(\chi_Z(\hat{Q}^2)\right)^2, \\ B^f &= - 2a_e e_f a_f \chi_Z(\hat{Q}^2) + 2v_e a_e 2v_f a_f \left(\chi_Z(\hat{Q}^2)\right)^2. \end{aligned} \quad (8)$$

The γZ interference and the pure Z exchange contain the reduced Z propagator

$$\chi_Z(Q^2) = \frac{Q^2}{Q^2 + M_Z^2}. \quad (9)$$

v_f and a_f are the vector and axial vector coupling constants of the fermions to the Z boson given by their charge e_f and isospin I_3^f:

$$v_f = \frac{I_3^f - 2s_W^2 e_f}{2s_W c_W}, \quad a_f = \frac{I_3^f}{2s_W c_W}. \quad (10)$$

The weak mixing angle is determined by the gauge boson masses ($c_W = \cos\theta_W$):

$$c_W = \frac{M_W}{M_Z}, \quad s_W^2 = 1 - c_W^2. \quad (11)$$

For Compton scattering we have

$$\frac{d^2\hat{\sigma}^{(0)}}{d\hat{x}d\hat{y}}(e\gamma \to e\gamma) = \frac{2\pi\alpha^2}{\hat{S}} \frac{1 + (1-\hat{y})^2}{1-\hat{y}} \delta(1-\hat{x}) \quad (12)$$

In leading logarithmic approximation the electromagnetic contributions to the parton distribution functions are generated by the evolution equation

$$Q^2 \frac{d}{dQ^2} D_{b/a}(z, Q^2) = \frac{\alpha(Q^2)}{2\pi} \int_z^1 \sum_{b'} \frac{d\beta}{\beta} P_{b/b'}(\beta) D_{b'/a}(z/\beta, Q^2). \quad (13)$$

To leading order the fragmentation function $\bar{D}_{a/b}(z)$ is equal to the parton density $D_{b/a}(z)$. The running fine structure constant is given by

$$\alpha(Q^2) \simeq \frac{\alpha(0)}{1 - (\alpha/3\pi)\sum_f e_f^2 \ln(Q^2/m_f^2)\Theta(Q^2 - m_f^2)}. \quad (14)$$

The Θ-function guarantees that only fermions with masses below Q^2 contribute to the running of α. $P(z)$ denote the Altarelli-Parisi splitting functions

$$P_{e/e}(z) = \frac{1+z^2}{(1-z)_+}, \quad (15)$$

$$P_{\gamma/q_f}(z) = \frac{1 + (1-z)^2}{z}, \quad (16)$$

and the (+)-distribution is defined by

$$\int_z^1 dz P_{e/e}(z) f(z) = \int_z^1 dz \frac{1+z^2}{1-z}(f(z) - f(1)) - \int_0^z dz \frac{1+z^2}{1-z} f(1). \quad (17)$$

2.1 First order corrections

$\mathcal{O}(\alpha)$ expressions for the structure functions are obtained from Eq. (13) supplementing it with the zeroth order initial condition $D_{a/b}^{(0)}(z) = \delta(1-z)\delta_{ab}$. For $D_{e/e}$ one finds:

$$D_{e/e}^{(1)}(z, Q^2) = \frac{\alpha}{2\pi} L_e P_{e/e}(z) \quad (18)$$

with

$$L_e = \ln \frac{Q^2}{m_e^2}. \quad (19)$$

In case of the photon distribution in the proton the initial values $D_{\gamma/P}(z,Q_0^2)$ at some reference momentum Q_0^2 could only be measured but not predicted with present theoretical techniques. To first order in α Eq. (13) can be rewritten as

$$D^{(1)}_{\gamma/P}(z,Q^2) = D_{\gamma/P}(z,Q_0^2) + \sum_f \frac{\alpha e_f^2}{2\pi}\int_{Q_0^2}^{Q^2}\frac{dQ'^2}{Q'^2}\int_z^1\frac{d\beta}{\beta}P_{\gamma/q_f}(\beta)D_{q_f/P}(z/\beta,Q'^2). \quad (20)$$

In the leading logarithmic approximation $D_{\gamma/P}(z,Q_0^2)$ should be ignored since it does not depend on two vastly differing mass scales (if Q_0^2 is chosen of the order of the proton mass) which would be required for a large logarithm. We use as approximate solution

$$D^{(1)}_{\gamma/P}(z,Q^2) \simeq \sum_f \frac{\alpha e_f^2}{2\pi}\ln\frac{Q^2}{Q_0^2}\int_z^1\frac{d\beta}{\beta}P_{\gamma/q_f}(\beta)D_{q_f/P}(z/\beta,Q^2). \quad (21)$$

which is obtained by neglecting the Q^2 dependence of the quark distributions in the Q'^2 integration of Eq. (20). Numerical calculations show that not neglecting this Q^2 dependence can change the final results for the Compton contribution to the eP cross section by about 10%. The same amount of uncertainty is found when the value of Q_0 is changed from 200 MeV to 400 MeV. This leads to errors in the final results for the $\mathcal{O}(\alpha)$ corrections of the order of 10 % only where the Compton part reaches the order of magnitude of the Born cross section, which is the case for small x and large y, *e.g.* at $x = 10^{-2}$ and $y \geq 0.96$ or at $x = 10^{-3}$ and $y \geq 0.93$. In this region the uncertainty in the results for the $\mathcal{O}(\alpha)$ corrections is dominated by the uncertainty of the photon distribution in the proton.

For the eP cross section, first order corrections are obtained from Eq. (3) by inserting the $\mathcal{O}(\alpha)$ result for one of the generalized densities, leaving for the others their initial values. The resulting three contributions to the differential cross section are visualized in Fig. 2. Inserting formula (18) into Eq. (3) we obtain a first contribution to the $\mathcal{O}(\alpha)$ radiative corrections describing initial state radiation from the electron

$$\left.\frac{d^2\sigma}{dxdy}\right|_i^{(1)} = \frac{\alpha}{2\pi}L_e\left\{\int_{z_1^{min}}^1 dz_1\frac{1+z_1^2}{1-z_1}\Big(\sigma_0(z_1,1)-\sigma_0(1,1)\Big) + S(z_1^{min})\sigma_0(1,1)\right\} \quad (22)$$

with

$$S(z) = 2\ln(1-z) + z + \frac{1}{2}z^2. \quad (23)$$

$$\sigma_0(z_1,z_3) = \frac{y}{z_1 z_3^2\hat{y}}\sum_{q_f}\int_0^1\frac{dz_2}{z_2}D_{q_f/P}(z_2,\hat{Q}^2)\frac{d^2\hat{\sigma}^{(0)}}{d\hat{x}d\hat{y}}(e^-q\to e^-q) \quad (24)$$

$$= \frac{2\pi\alpha^2 y}{z_1 z_3^2\hat{y}^3\hat{S}}\sum_{q_f}D_{q_f/P}(\tilde{z}_2,\hat{Q}^2)\Big(A^f[1+(1-\hat{y})^2] \pm B^f[1-(1-\hat{y})^2]\Big)\Big|_{z_2=\tilde{z}_2}$$

$$\tilde{z}_2 = \frac{z_1 x y}{z_1 z_3 + y - 1}, \quad (25)$$

and

$$z_1^{min} = \frac{1-y}{1-xy}. \quad (26)$$

Besides kinematical factors, σ_0 is just the Born expression for electron proton scattering with appropriately rescaled variables $(x,y,Q^2 \to \hat{x},\hat{y},\hat{Q}^2)$.

The corresponding expression for $\mathcal{O}(\alpha)$ final state radiation from the electron reads

$$\left.\frac{d^2\sigma}{dxdy}\right|_f^{(1)} = \frac{\alpha}{2\pi}L_e\left\{\int_{z_3^{min}}^1 dz_3\frac{1+z_3^2}{1-z_3}\Big(\sigma_0(1,z_3)-\sigma_0(1,1)\Big) + S(z_3^{min})\sigma_0(1,1)\right\} \quad (27)$$

with

$$z_3^{min} = 1 - y(1-x). \quad (28)$$

For the Compton contribution we find from Eq. (3) and using Eq. (21)

$$\left.\frac{d^2\sigma}{dxdy}\right|_C^{(1)} = \int\frac{dz_2}{z_2}D^{(1)}_{\gamma/P}(z_2,Q^2)\left.\frac{d\hat{\sigma}^{(0)}}{d\hat{x}d\hat{y}}(e\gamma\to e\gamma)\right|_{z_1=z_3=1} = \frac{2\pi\alpha^2}{xS}\frac{1+(1-y)^2}{1-y}D^{(1)}_{\gamma/P}(x,Q^2) \quad (29)$$

Although this part does not contain a logarithm of the electron mass, it should not be neglected because it increases with an inverse power $1/(1-y)$ as $y \to 1$. In an exact $\mathcal{O}(\alpha)$ calculation of the leptonic corrections shown in Fig. 1 it is automatically included. The results of Eqs. (22), (27), and (29) agree with those of [4,5].

2.2 Second order corrections

2.2.1 Two photon radiation from the electron line

Inserting the $\mathcal{O}(\alpha)$ results for the electron structure function into the evolution equation Eq. (13) one can determine a first contribution to the diagonal electron density in $\mathcal{O}(\alpha^2)$:

$$D^{(2\gamma)}_{e/e}(z,Q^2) = \frac{1}{2}\left(\frac{\alpha}{2\pi}\right)^2 L_e^2\int_z^1\frac{d\beta}{\beta}P_{e/e}(\beta)P_{e/e}(\beta/z). \quad (30)$$

After evaluating the integral in the last equation and inserting the result into Eq. (3) the contribution of $\mathcal{O}(\alpha^2)$ two-photon initial state radiation from the electron (Fig. 3a)

may be written as

$$\left.\frac{d^2\sigma}{dxdy}\right|_{\gamma}^{(2)} = \frac{1}{2}\left(\frac{\alpha}{2\pi}\right)^2 L_e^2 \left\{\int_{z_1^{min}}^1 dz_1 \left[2\frac{1+z_1^2}{1-z_1}\left(2\ln(1-z_1)-\ln(z_1)+\frac{3}{2}\right)\right.\right.$$
$$\times\left(\sigma_0(z_1,1)-\sigma_0(1,1)\right)$$
$$\left.+\left((1+z_1)\ln z_1 - 2(1-z_1)\right)\sigma_0(z_1,1)\right]$$
$$+\left\{\left[S(z_1^{min})\right]^2 + 4\mathrm{Li}_2(1-z_1^{min}) + z_1^{min}(z_1^{min}-2)\ln z_1^{min}\right.$$
$$\left.\left.-\frac{1}{4}(z_1^{min})^4 - (z_1^{min})^3 - (z_1^{min})^2 - z_1^{min} + \frac{13}{4}\right\}\sigma_0(1,1)\right\}. \tag{31}$$

The corresponding expression for final state radiation (Fig. 3b) is determined by the same expression with the replacement

$$z_1^{min}, \sigma_0(z_1,1) \to z_3^{min}, \sigma_0(1,z_3). \tag{32}$$

The contribution from initial-final state interference (Fig. 3c) is obtained by inserting the $\mathcal{O}(\alpha)$ contributions to both the electron density $D_{e/e}^{(1)}(z_1)$ and the fragmentation function $\tilde{D}_{e/e}^{(1)}(z_3)$ in Eq. (3). The result can be written in the form

$$\left.\frac{d^2\sigma}{dxdy}\right|_{int}^{(2)} = \left(\frac{\alpha}{2\pi}\right)^2 L_e^2 \left\{\int_{z_1^{min}}^1 dz_1 \frac{1+z_1^2}{1-z_1}\left[\tau(z_1)-\tau(1)\right.\right.$$
$$\left.+S(z_3^{min}(z_1))\left(\sigma_0(z_1,1)-\sigma_0(1,1)\right)\right]$$
$$+\int_{z_3^{min}}^1 dz_3 \frac{1+z_3^2}{1-z_3}\left(\sigma_0(1,z_3)-\sigma_0(1,1)\right)S(z_1^{min}) \tag{33}$$
$$+\int_{z_1^{min}}^1 dz_1 \frac{1+z_1^2}{1-z_1}\left(S(z_3^{min}(z_1))-S(z_3^{min})\right)\sigma_0(1,1)$$
$$\left.+S(z_1^{min})S(z_3^{min})\sigma_0(1,1)\right\}.$$

with

$$\tau(z_1) = \int_{z_3^{min}(z_1)}^1 dz_3 \frac{1+z_3^2}{1-z_3}\left(\sigma_0(z_1,z_3)-\sigma_0(z_1,1)\right) \tag{34}$$

and

$$z_3^{min}(z_1) = \frac{z_1 xy + 1 - y}{z_1}. \tag{35}$$

Another second order contribution describing two-photon emission from the electron line is obtained as $\mathcal{O}(\alpha)$ leptonic corrections to the Compton part of the $\mathcal{O}(\alpha)$ corrections (Fig. 3d). This contribution is derived with the help of the $\mathcal{O}(\alpha)$ expressions Eq. (18) for the electron density and the electron fragmentation function

applying the same formalism to the $e\gamma \to e\gamma$ subprocess. The resulting contributions to the differential ep cross section have the same structure as the $\mathcal{O}(\alpha)$ leptonic corrections for initial and final state radiation, Eqs. (22) and (27), resp., provided that the lowest order cross section $\sigma_0(z_1,z_3)$ of Eq. (24) is replaced by the corresponding expression for the Compton part of the $\mathcal{O}(\alpha)$ corrections Eq. (29).

$$\begin{aligned}\sigma_C(z_1,z_3) &= \frac{y}{z_1 z_3^2 \hat{y}}\int_0^1 \frac{dz_2}{z_2} D_{\gamma/P}^{(1)}(z_2,\hat{Q}^2)\frac{d^2\hat{\sigma}^{(0)}}{d\hat{x}d\hat{y}}(\epsilon^-\gamma \to \epsilon^-\gamma) \\ &= \frac{y}{z_1 z_3^2 \hat{y}} D_{\gamma/P}^{(1)}(\tilde{z}_2,\hat{Q}^2)\frac{2\pi\alpha^2}{\hat{S}}\frac{1+(1-\hat{y})^2}{1-\hat{y}},\end{aligned} \tag{36}$$

with $\tilde{z}_2$ from Eq. (25). The order of magnitude of the resulting second order contribution is determined by $(\alpha/2\pi)^2 L_e \ln(Q^2/Q_0^2)$.

2.2.2 Fermion pair production from the electron line

Additional fermion-pairs come from two sources (Figs. 3e, f). Direct fermion pair production (Fig. 3e) combined with the diagram describing a photon self energy insertion in the one-loop vertex correction can be respected by the use of the running coupling constant Eq. (14) in the evolution equations to second order. This corresponds to the replacement

$$\frac{\alpha}{2\pi}\ln\frac{Q^2}{m_e^2} \longrightarrow \frac{\alpha}{2\pi}\ln\frac{Q^2}{m_e^2} + \frac{1}{3}\sum_f e_f^2\left(\frac{\alpha}{2\pi}\ln\frac{Q^2}{m_f^2}\right)^2\Theta(Q^2-m_f^2) \tag{37}$$

in the $\mathcal{O}(\alpha)$ contributions and results in

$$D_{e/e}^{f\bar{f}}(z) = \frac{1}{3}\sum_f e_f^2\left(\frac{\alpha}{2\pi}\ln\frac{Q^2}{m_f^2}\right)^2\Theta(Q^2-m_f^2)P_{e/e}(z). \tag{38}$$

The other source is the hard scattering of the electron from a produced e^+e^- pair (Fig. 3f). In QCD language this corresponds to a sea contribution. A similar situation occurs for the fragmentation of the final state electron. The corresponding term in the second order electron density is obtained by iterating the evolution equation Eq. (13) twice, with the kernels $P_{\gamma/e}$ and $P_{e/\gamma}$:

$$D_{e/e}^{e^+e^-}(z,Q^2) = \left(\frac{\alpha}{2\pi}\ln\frac{Q^2}{m_e^2}\right)^2\left[(1+z)\ln z + \frac{1}{2}(1-z) + \frac{2}{3}\frac{1-z^3}{z}\right]. \tag{39}$$

These results are in agreement with Ref. [9]. The important point to realize is the occurence of a $1/z$ term characteristic for a sea distribution.

The complete result for the electron structure function to second order is

$$D_{e/e}^{(2)} = D_{e/e}^{2\gamma} + D_{e/e}^{f\bar{f}} + D_{e/e}^{e^+e^-}. \tag{40}$$

Together with the contribution from initial-final state interference and the leptonic corrections to the Compton part this determines the complete $\mathcal{O}(\alpha^2)$ corrections in leading logarithmic approximation.

3. Numerical Results and Discussion

In this section we present numerical results for first and second order corrections to electron proton scattering based on the formulas of the previous section[2]. Fig. 4 shows a comparison of the $\mathcal{O}(\alpha)$ leading leptonic corrections with the corrections including also the $\mathcal{O}(\alpha^2)$ contributions. In this and the following figures we have used the quark distribution functions of Ref. [13] and $M_W = 80.0\,GeV$, $M_Z = 91.1\,GeV$. The hadronic mass scale in the photon distribution function Eq. (21) was chosen to be $Q_0 = 200\,MeV$.

The features of the $\mathcal{O}(\alpha)$ corrections are:

- At large x and small y the combined contributions of virtual and real soft photons lead to large negative corrections. These are described by $S(z_i^{min})$ in Eq. (22) and (27). They factorize from the lowest order cross section. For $y \to 0$ one finds $z_i^{min} \to 1$ and the log term in S becomes large. In the region where this term is dominating, the corrections are insensitive to the details of the parton distribution functions and the weak interaction parameters.

  However, at small x, the non-factorized parts in Eqs. (22) and (27) are important even in the limit $y \to 0$. For small y, energy-momentum conservation restricts the energy of bremsstrahlung photons to small values compared to the electron energy in this case. But these photons must be considered as hard photons because their energy is large enough to induce a large variation of the underlying non-radiative cross section. The non-factorized parts in Eqs. (22) and (27) are very sensitive to the shape of the parton distribution functions. In particular, they are responsible for the increase of the corrections with $y \to 0$ at small x.

- The corrections are large for $y \to 1$, especially at small x, due to emission of photons with high energy which shifts the momentum transfer to small values. Not only emission into the forward direction but also the Compton part is increasingly important with increasing y. Both contributions behave like $1/(1-y)$ with y going to 1. Already at $x = 0.1$, $y = 0.9$ the $\mathcal{O}(\alpha)$ corrections reach the 50% level.

It is seen in Fig. 4 that the $\mathcal{O}(\alpha^2)$ corrections are also large for large x and small y. They are even larger and certainly non-negligible in the small x - large y region (see Fig. 5b). For $x = 10^{-2}$, $y = 0.95$ the $\mathcal{O}(\alpha^2)$ corrections reach 30%.

[2]The results presented here do not include self energy corrections to the gauge boson propagators although these provide another source of large logarithms and should be included in a complete calculation of radiative corrections.

In order to discuss the origin of the $\mathcal{O}(\alpha^2)$ corrections we present in Fig. 5 results for the separate contributions. There it can be seen that the large $\mathcal{O}(\alpha^2)$ contributions at large x are due to the direct 2γ parts of Eqs. (31, 32, 33). An inspection of the formulae reveals that it is essentially the soft part $[\sum_i S(z_i^{min})]^2/2$ which leads to positive contributions at small y. In the small x region, however, the main effect comes again from hard radiation, first of all by additional e^+e^- pairs Eq. (39). This contribution increases like $1/x(1-y)^2$. Also the $\mathcal{O}(\alpha^2)$ contribution to the Compton part Eq. (36) gets large at small x and large y.

For large x and small y the hard contribution is small and the behavior of the corrections is essentially determined by the soft contribution $\propto S(z_i)\ln(Q^2/m_e^2)$. Exponentiation of these IR parts [14,15] would improve the predictions for the cross section. The exponentiation of these terms can in fact be derived by an iterative solution of the evolution equation Eq. (13). The full prescription of [14] would include in addition to this also IR contributions not proportional to a large logarithm. However, at large y, especially for small x the corrections are mainly due to hard photon and fermion pair emission and exponentiation of the soft part does not lead to an inclusion of the dominant higher order corrections.

We stress again that the large positive corrections are due to the fact that the corrections include cross sections for new processes, *i.e.* one-photon, two-photon, and fermion pair production. These new processes are integrated over the whole phase space available to the additional photons, fermions, resp. because an analytical calculation with cuts is in general much too complicated. These contributions should not be included as corrections if they can be separated experimentally.

There are several possibilities to identify experimentally events of these new types:

- Large angle emission of photons can be directly observed, unless the photon is inside a jet. In the latter case it is probably not possible to separate photons from decays of hadrons. Events of this type are, however, expected to be rare. Cutting out events with a high p_T photon will reduce the bremsstrahlung cross section. Especially the Compton part (Eq. (29)) will be eliminated by such a cut leading to a considerable decrease of the corrections at small x and large y.

- To some extent, photons coming close to the electron direction will be seen in the H1 and ZEUS experiments at HERA with the help of a forward detector, originally designed for luminosity measurements. These detectors will cover the range of polar angle up to about 1 *mrad*. This will reduce but not remove the large y peak in the correction.

- There is also the possibility to indirectly identify events with additional photons or fermion pairs by comparing the measured current jet angle with the one

expected from the electron measurement. Measuring the momentum of the scattered electron and assuming that the basic scattering process is a $2 \to 2$ process one can determine via x and Q^2 the angle and the energy of the scattered quark. In case of γ emission, the momentum of the scattered quark depends also on the energy and the emission angle of the bremsstrahlung photon. If the photon is emitted collinearily with the incoming electron, one finds:

$$\cos\theta_{q'} = \frac{(y+z_1-1)^2 E_e - xy(1-y)E_P}{(y+z_1-1)^2 E_e + xy(1-y)E_P}, \qquad E_{q'} = E_e(y+z_1-1) + \frac{xy(1-y)}{y+z_1-1}E_P \tag{41}$$

where E_P and E_e are the energies of the proton and the electron and $z_1 = 1 - E_\gamma/E_e$ (see Eq. (4)). $\theta_{q'}$ is defined with respect to the elctron beam direction. In Fig. 6 we show the effect of emission of a photon collinear with the incoming electron on the energy and the polar angle of the scattered quark (which is closely related to the energy and angle of the current jet). It is important that the polar angle $\theta_{q'}$ is always increasing with the photon energy. This also means that for very small values of x where according to the non-radiative kinematics one can not expect the jet to be fully contained in the detector, photon emission will turn the jet to larger angles.

In Fig. 7 we demonstrate the influence of a cut for the difference of the true and expected quark scattering angles

$$\Delta\theta_{q'} = \theta_{q'} - \theta_{q'}(z_1 = 1)$$

on the $\mathcal{O}(\alpha)$ corrections. Using Eq. (41), the condition $\Delta\theta_{q'} \geq \Delta$ restricts the range of integration over z_1 for initial state radiation and thus reduces the corrections. In these figures the dashed lines show the corrections where besides a cut on $\Delta\theta_{q'}$ also the Compton part is left out (because this part is always characterized by events with a photon of large transverse momentum). In addition to this also the final state emission is reduced with the help of a cut on the photon energy of $2\,GeV$. The corrections come out to be always flat functions of y of the order of $0\,\%$ to $-20\,\%$. The step-like behavior at small y is due to the fact that the cut on the photon energy for final state radiation becomes active only above a certain threshold in y. The dependence on the actual value of Δ is not strong (see Fig. 7b). Therefore, it is not required to determine the jet axis to high precision. An accuracy of the order of 15 degrees would be sufficient, although the jet axis can in fact be determined with much higher precision (few degrees). In Fig. 8 results of a similar calculation for $S = 1.6 \times 10^6\,GeV^2$ are shown.

The effect of cuts of these types have also been studied using the Monte Carlo event generator HERACLES. The results obtained with HERACLES confirm the conclusions found here and will be published in a forthcoming paper [6].

Of course, these results only indicate the potentiality of reducing the radiative corrections by suitable cuts. We have passed over a discussion of the actual feasibility of the cuts, but we believe that experimental details will only change the final amount of the reduction but not the conclusion on principle. A full study needs the inclusion of fragmentation effects and must also take into account the properties of the detectors.

In summary, we have shown that $\mathcal{O}(\alpha^2)$ electromagnetic corrections are significant in some regions of the accessible phase space, and cannot be ignored. The origin of these relatively large terms is well understood. From this point of view we do not expect large contributions neither from higher order leading terms $\mathcal{O}((\alpha/\pi)^3 \ln^3(Q^2/m^2)) \simeq 3 \times 10^{-4}$, nor from non-leading logarithms[3]. Uncertainties in the calculation of theoretical predictions for the deep inelastic electron-proton scattering cross section are thus not due to an insufficient knowledge of higher order electroweak radiative corrections but the reliability of predictions is limited by the precision with which hadronic structure functions (especially $D_{\gamma/P}$) are known. In this sense one could say that the limit where radiative corrections are under control has been shifted to much larger y and smaller x. However, more work is required to study combined effects of strong and electromagnetic corrections.

As a main point of our analysis we have shown that the huge radiative corrections can be reduced dramatically by appropriate experimental cuts.

References

[1] Proceedings of the HERA Workshop, Hamburg 1987, ed. R. D. Peccei, Vol. 1 and 2.

[2] D. Yu. Bardin, C. Burdik, P. Ch. Christova, T. Riemann, Dubna preprint E2-87-595, E2-88-682, and Z. Phys. C 42 (1989) 679.

[3] M. Böhm, H. Spiesberger, Nucl. Phys. B 294 (1987) 1081.

[4] W. Beenakker, F. A. Berends, W. L. van Neerven, Proceedings of the Ringberg Workshop on "Radiative Corrections for e^+e^- Collisions", Ringberg 1989, ed. J. H. Kühn, p.3.

[5] J. Blümlein, Z. Phys. C 47 (1990) 89.

[3] Corrections of order $\mathcal{O}(\alpha^2 \ln(Q^2/m^2))$ have been calculated in [9].

[6] A. Kwiatkowski, H.-J. Möhring, H. Spiesberger, DESY 90-041, 1990; and in preparation.

[7] V. N. Gribov and L. N. Lipatov, Sov. J. Nucl. Phys. 15 (1972) 438, 675.

[8] G. Altarelli, G. Parisi, Nucl. Phys. B 126 (1977) 298.

[9] E. A. Kuraev, N. P. Merenkov, V. S. Fadin, Sov. J. Nucl. Phys. 47 (1988) 1009.

[10] "Z Physics at LEP1", Eds. G. Altarelli, R. Kleiss, and C. Verzegnassi, CERN report 89-08 (1989).

[11] J. Kripfganz, H.-J. Möhring, Z. Phys. C 38 (1988) 653.

[12] J. Kripfganz, H.-J. Möhring, KMU-HEP 89-04 Internal Report, February 1989.

[13] P. N. Harriman, A. D. Martin, R. G. Roberts, W. J. Stirling, preprint RAL-90-007 (1990).

[14] D. R. Yennie, S. C. Frautschi, H. Suura, Ann. of Physics 13 (1961) 379.

[15] M. Consoli, M. Greco, Nucl. Phys. B 186 (1981) 519.

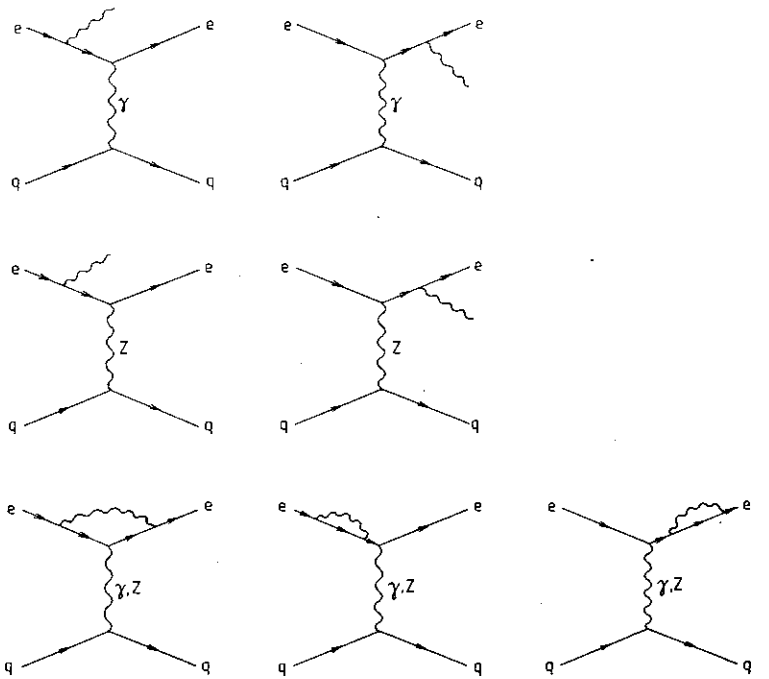

Figure 1: Feynman diagrams for $\mathcal{O}(\alpha)$ leptonic QED corrections to $eq_f \to eq_f$.

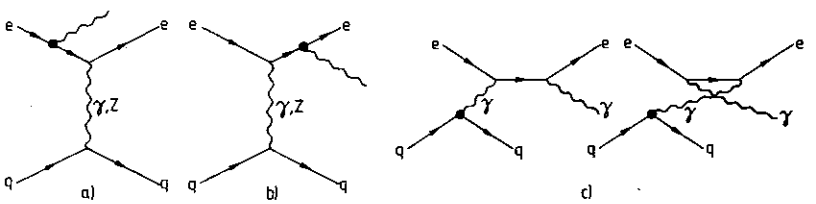

Figure 2: First order leading logarithmic corrections to $eq_f \to eq_f$ arising from the diagrams of Fig. 1. The vertices emphasized by a bold point describe $\mathcal{O}(\alpha)$ mass singularities contained in structure functions.

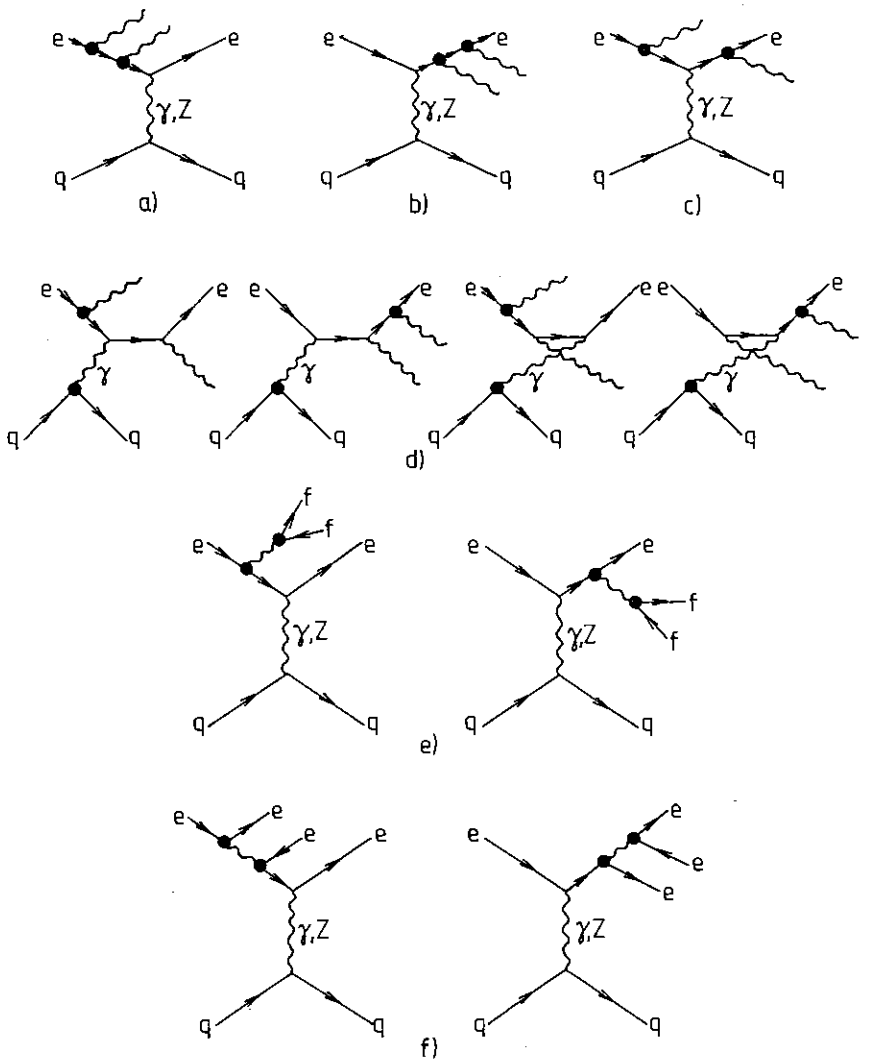

Figure 3: Second order leading logarithmic corrections to $eq_f \to eq_f$ using the same conventions as in Fig. 2.

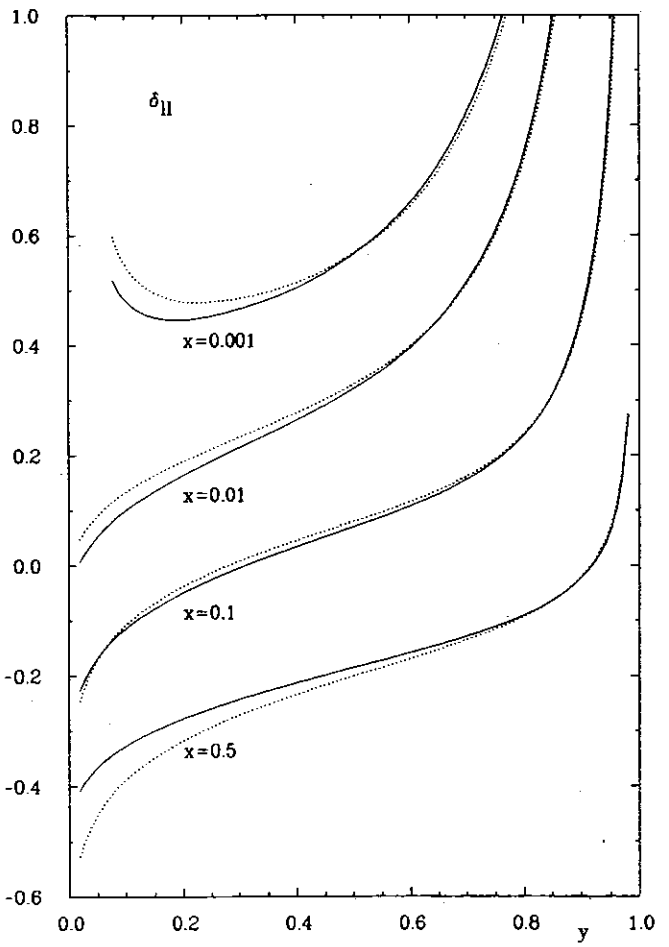

Figure 4: Leptonic corrections for $e^- p \to e^- X$ at $S = 10^5\, GeV^2$ in the leading logarithmic approximation for $x = 0.5$, $x = 0.1$, $x = 0.01$, and $x = 0.001$. The dotted curves show the $\mathcal{O}(\alpha)$ results and the full curves include also the $\mathcal{O}(\alpha^2)$ contributions from Eqs. (31, 32, 33, 36, 38, 39). ($M_W = 80.0\, GeV$, $M_Z = 91.1\, GeV$, $Q_0 = 200\, MeV$, quark distributions from [13]).

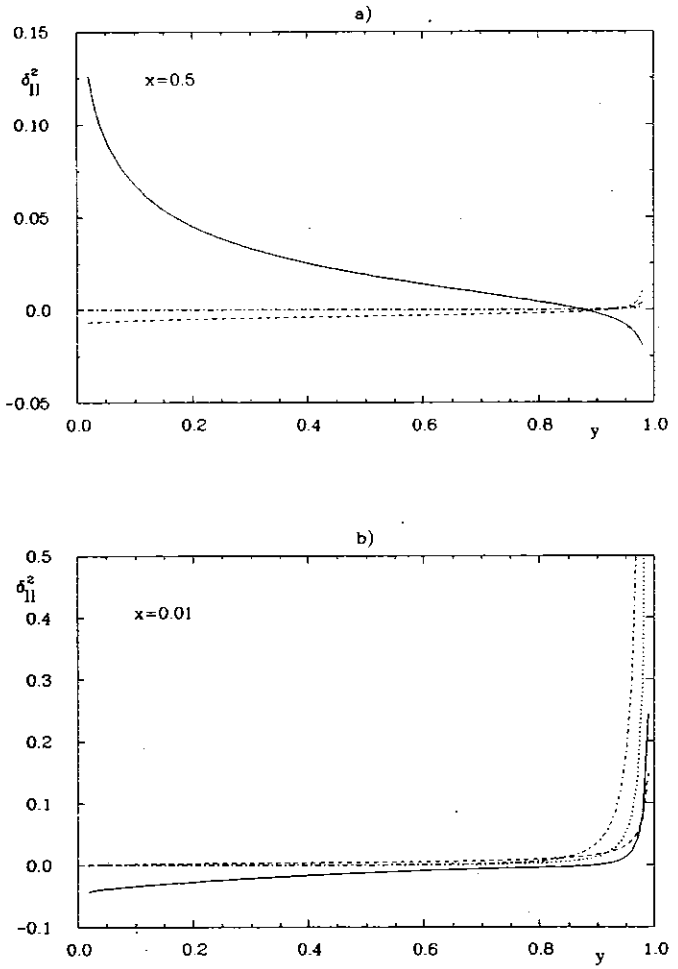

Figure 5: Separate contributions to the $\mathcal{O}(\alpha^2)$ leading leptonic corrections for $S = 10^5\,GeV^2$, $x = 0.5$, and $x = 0.01$. The full line contains the 2γ contributions from Eqs. (31, 32, 33), the dotted curve shows the 2γ part from Eq. (36) (Compton scattering), the dashed line is for the $f\bar{f}$ contribution (Eq. (38)), and the effect of additional e^+e^- pairs (Eq. (39)) is represented by the dashed-dotted line. ($M_W = 80.0\,GeV$, $M_Z = 91.1\,GeV$, $Q_0 = 200\,MeV$, quark distributions from [13]).

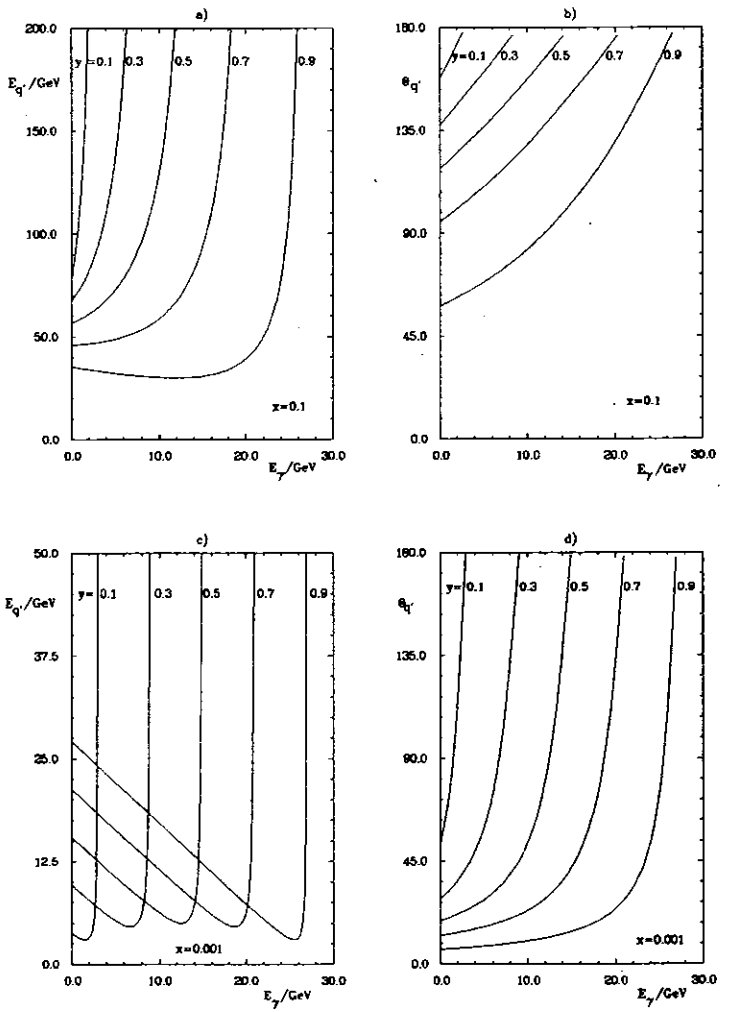

Figure 6: Dependence of the energy (a and c) and the polar angle (b and d) of the scattered quark on the photon energy in case of photon emission collinear with the incoming electron. a) and b) for $x = 0.1$, c) and d) for $x = 0.001$. $E_e = 30\,GeV$, $E_P = 820\,GeV$.

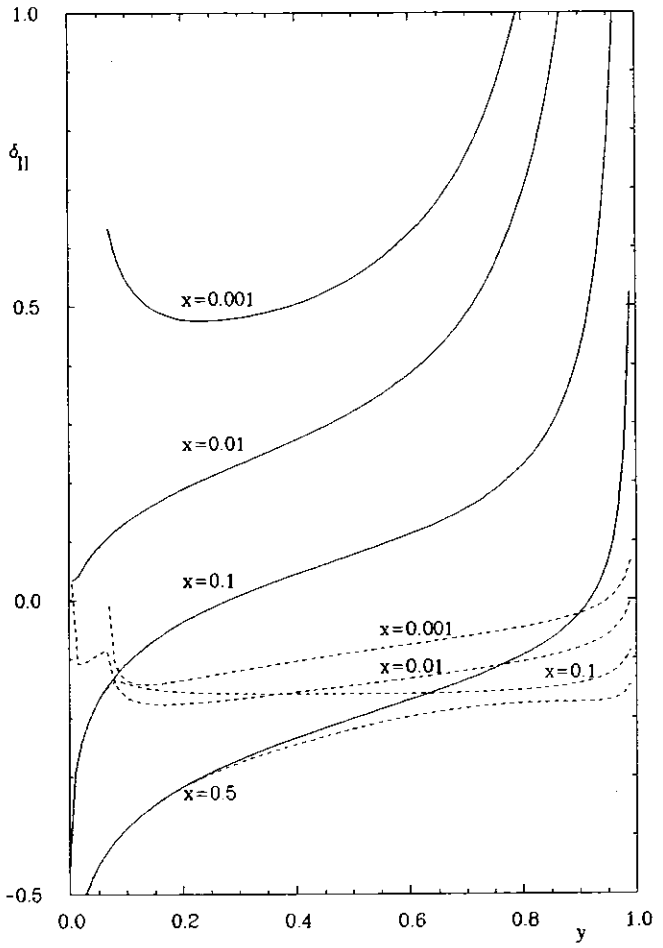

Figure 7a: Reduction of the $\mathcal{O}(\alpha)$ leptonic corrections by a cut on the difference of the true and expected quark scattering angle for $x = 0.001$, $x = 0.01$, $x = 0.1$, and $x = 0.5$. The full lines are the complete $\mathcal{O}(\alpha)$ results for $S = 10^5\, GeV^2$ without cut and the dashed lines for a cut of $\Delta = 15^o$. ($E_\gamma \leq 2\, GeV$ for final state emission.)

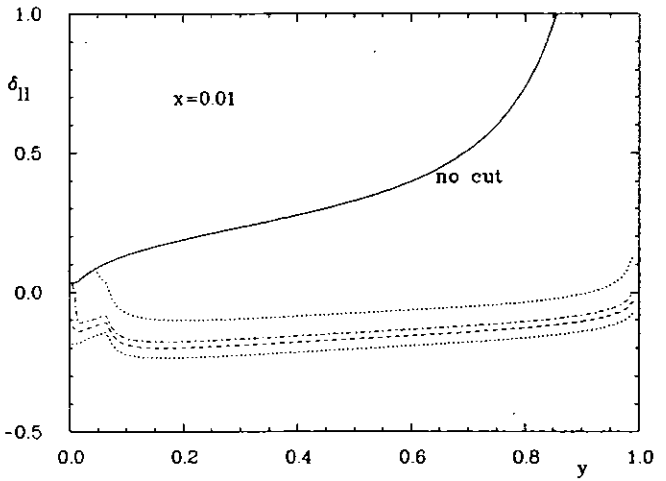

Figure 7b: Reduction of the $\mathcal{O}(\alpha)$ leptonic corrections by a cut on the difference of the true and expected quark scattering angle for $x = 0.01$ and $\Delta = 5^o$ (lower dotted curve), 10^o (dashed curve), 15^o (dashed-dotted curve), and 45^o (upper dotted curve). ($E_\gamma \leq 2\, GeV$ for final state emission.)

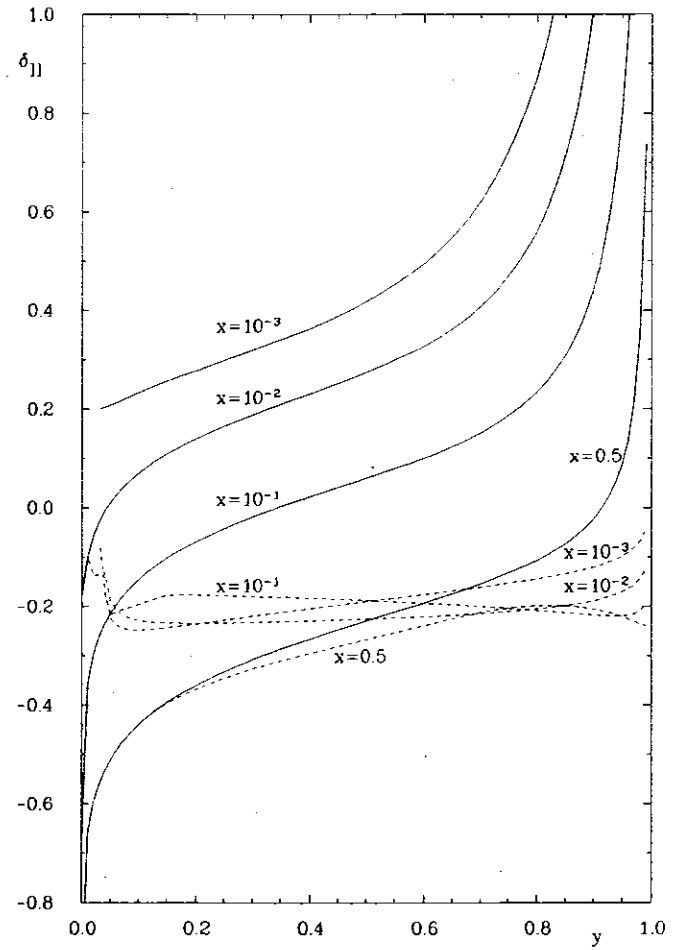

Figure 8: Same as Fig. 7a, but for $S = 1.6 \times 10^6\ GeV^2$.